Theoret. Chim. Acta (Berl.) 56, 269–296 (1980)

THEORETICA CHIMICA ACTA

Chemical Applications of Group Theory and Topology

VIII. Topological Aspects of Oscillating Chemical Reactions [1]

R. Bruce King

Department of Chemistry, University of Georgia, Athens, Georgia 30602, U.S.A.

The following procedure is described for investigating the qualitative dynamics of simple chemical systems: 1) A so-called influence diagram is generated representing the relationships between the reference reactants (phase-determining intermediates); 2) This influence diagram is used to generate a "truth table" indicating possible transitions between state vectors representing the signs of the time derivatives of of the reference reactant concentrations; 3) The truth table is used to determine a state transition diagram representing the flow topology around unstable equilibrium points; 4) The characteristic equation of the adjacency matrix of the influence diagram is solved in order to determine the presence of such unstable equilibrium points. The two types of qualitative dynamics possible for chemical systems containing two reference reactants and one feedback circuit are bifurcation between two attracting regions (bistability) and limit cycle oscillation. However, in two reference reactant systems oscillation requires an additional self-activating loop to generate the unstable equilibrium point required for its realization. Bistability and limit cycle oscillation are also two of the possible types of qualitative dynamics for chemical systems containing three reference reactants. However, chemical systems with three reference reactants and two or more feedback circuits can also contain interlocking limit cycles, which can lead to toroidal oscillations or chaos. The influence diagrams are given for the systems exhibiting these various types of dynamic behavior along with a summary of the important properties of all 729 possible influences for simple chemical systems containing three reference reactants.

Key words: Group theory, chemical applications of ~ – Topology, chemical applications of ~ – Oscillating chemical reactions, topological aspects of ~.

1. Introduction

The first example of a homogeneous chemical reaction system exhibiting oscillatory behavior was the iodate-hydrogen peroxide system discovered by

0040–5744/80/0056/0269/$05.60

Bray in 1921 [2, 3]. However, extensive interest in chemical oscillations only developed after the discovery by Belousov [4] of a system containing citric acid, cerium (IV), and bromate in acidic aqueous solution which exhibits highly reproducible periodic behavior. Subsequent work by Zhabotinskii [5, 6] led to minor modifications of the reactants (e.g. substitution of other brominatable compounds for the citric acid such as malonic acid) which resulted in improved oscillatory behaviour so that this reaction is now known as the Belousov–Zhabotinskii reaction. Since then oscillatory chemical reactions have been studied extensively both experimentally and theoretically [7, 8, 9] particularly because of their value as models for important biological phenomena [10] including nerve and muscle action, cell respiration, mitosis, morphogenesis, and regeneration of damaged cells. Still more recently Rössler has begun to develop the theory of chemical systems exhibiting still more exotic kinetics including toroidal (biperiodic) oscillations [11] and nonperiodic oscillations ("chaos") [11, 12, 13, 14].

Despite all of this extensive recent research, both experimental and theoretical, in oscillating chemical reactions, no progress has been made in developing methods to synthesize real homogeneous chemical oscillatory behavior. Thus the known homogeneous chemical oscillators, including the Bray–Liebhafsky iodate/hydrogen peroxide [2, 3] and the Belousov–Zhabotinskii bromate/malonic acid/cerium (IV) [4, 5, 6] systems, were discovered by accident. Elegant experimental work mainly by Noyes and co-workers [15, 16, 17] has elucidated the salient features of the kinetics and mechanisms of such chemical oscillators. Equally elegant applied mathematical techniques have been used to analyze theoretically the dynamics of specific systems [10]. However, the general pattern of most of the experimental and theoretical work has been to examine specific dynamic systems in great detail with much less attention being given to the total scope of the possibilities for dynamic systems exhibiting oscillatory behaviour. More general treatments of oscillating reactions include a 1967 paper by Higgins [18] and a 1973 paper by Tyson and Light [19]. However, both papers are limited to two-component systems (i.e. systems with two phase-determining intermediates in the terminology below). Attempts to extend these treatments to systems containing three or more components lead to considerable difficulties.

This paper describes a technique based on switching circuit theory [20] and several recent papers by Glass [21, 22, 23, 24, 25] for uncovering some important qualitative features of the dynamics of relatively complicated chemical systems, particularly those undergoing oscillations of various types. This treatment involves an exhaustive analysis of all dynamic systems of a given type at considerable expense in the quantitative treatment of a specific system.

2. General Background

The species found in chemical oscillators can be classified as major reactants, reference reactants, and derived reactants with the following characteristics [16, 17].

1) Major reactants: The major reactants are consumed irreversibly to generate the free energy change that drives the oscillatory system. Their variations during a single cycle of oscillation represent only small fractions of their total concentrations. For this reason an approximate description of a chemical oscillator can regard the concentrations of the major reactants as almost constant during the period of a single oscillation. For example, the major reactants in the Belousov–Zhabotinskii reaction are bromate and malonic acid [16].

2) Reference reactants: In a chemical oscillator the concentrations of the reference reactants provide sufficient information to define the position of the system along the trajectory of its oscillations as a point in n-dimensional space ("concentration space") where n is the number of reference reactants and the coordinates correspond to the concentrations of each reactant. The necessarily positive concentrations of the reference reactants are mutually independent so that any point in the positive octant of the concentration space is potentially accessible. The reference reactants in chemical oscillators have also been called *phase-determining intermediates* [17], *phase variables*, and *state variables* in various papers. The reference reactants in the Belousov–Zhabotinskii reaction are bromous acid, bromide, and cerium (IV) [16].

3) Derived reactants: The concentrations of the derived reactants are generally much less than those of the reference reactants. Furthermore, the concentrations of the derived reactants cannot be varied independently from those of the reference reactants. Examples of derived reactants in the Belousov–Zhabotinskii reaction are BrO_2, HOBr, and Br_2 [16].

This paper discusses the properties of chemical reaction systems containing three reference reactants which will be designated X, Y, and Z throughout the paper. The position of the system can thus always be defined by a point in the positive actant of three-dimensional space (R^3). An *equilibrium point* of such a three reference reactant system is defined by Eq. (1)

$$\dot{X} = \dot{Y} = \dot{Z} = 0 \tag{1}$$

where the dots refer to the time derivatives dX/dt, dY/dt, and dZ/dt, respectively. Such an equilibrium point is *stable* if all nearby solutions stay nearby for all future time [26]. In the case of a two-dimensional system where a third dimension represents energy (mathematically a Liapunov function [26], which can never decrease), a stable equilibrium represents a pit and an unstable equilibrium represents a peak. In order to evaluate the stability of an equilibrium point in a three-dimensional system, the following determinantal equation must be solved:

$$\begin{vmatrix} \left(\frac{\partial \dot{X}}{\partial X}\right)_0 - \lambda & \left(\frac{\partial \dot{X}}{\partial Y}\right)_0 & \left(\frac{\partial \dot{X}}{\partial Z}\right)_0 \\ \left(\frac{\partial \dot{Y}}{\partial X}\right)_0 & \left(\frac{\partial \dot{Y}}{\partial Y}\right)_0 - \lambda & \left(\frac{\partial \dot{Y}}{\partial Z}\right)_0 \\ \left(\frac{\partial \dot{Z}}{\partial X}\right)_0 & \left(\frac{\partial \dot{Z}}{\partial Y}\right)_0 & \left(\frac{\partial \dot{Z}}{\partial Z}\right)_0 - \lambda \end{vmatrix} = 0. \tag{2}$$

In this equation the zero subscripts refer to the values of the indicated partial derivatives at the equilibrium point being evaluated.

Expanding the determinant in Eq. (2) gives a cubic polynomial characteristic equation:

$$A\lambda^3 + B\lambda^2 + C\lambda + D = 0. \tag{3}$$

For a given equilibrium point to be stable all solutions λ of the corresponding characteristic polynomial (Eq. (3)) must have a negative real part. Existence of even one solution of Eq. (3) with a positive real part is sufficient to indicate instability of the corresponding equilibrium point [27].

Stable equilibrium points are clearly significant in indicating where a dynamic system, including a chemical one, will come to rest. The significance of unstable equilibrium points in determining dynamic behavior is not as obvious and depends upon the neighborhood around the unstable equilibrium point (i.e. the topology). This paper provides a method for evaluating the topology around unstable equilibrium points in chemical systems to obtain information concerning their dynamic behavior. A method for determining the existence of unstable equilibrium points based on the above principles is also presented.

3. Systems with Two Reference Reactants

Some of these concepts can be clarified by considering a chemical system containing two reference reactants X and Y with the following provisions: 1) Only unimolecular and bimolecular reactions are allowed in accord with what is chemically reasonable; 2) The concentrations of all reactants other than the reference reactants X and Y are incorporated into the rate constants; since all concentrations are positive, the signs of these rate constants are not affected by this provision; 3) All rate constants are defined in such a way that they are positive. Under such conditions Tyson and Light [19] have derived the following expressions:

$$\dot{X} = k_0 \pm k_1 X + k_2 Y - k_3 X^2 \pm k_4 XY + k_5 Y^2 \tag{4a}$$

$$\dot{Y} = c_0 \pm c_1 Y + c_2 X - c_3 Y^2 \pm c_4 YX + c_5 X^2 \tag{4b}$$

where the permissible signs of the terms are determined as follows:

1) k_0, k_2, k_5, c_0, c_2, and c_5 are positive since a chemical species can only disappear at a rate proportional to a non-zero power of its concentration (otherwise concentrations could become negative – obviously unreasonable).
2) k_3 and c_3 are negative because the restriction to unimolecular and bimolecular processes requires these rate constants to correspond to processes destroying X and Y, respectively.

In Eqs. (4a) and (4b) a term with a positive sign corresponds to an activating step and a term with a negative sign corresponds to an inhibiting step. At an equilibrium point (steady state) $\dot{X} = \dot{Y} = 0$ leading to

$$0 = k_0 \pm k_1 X + k_2 Y - k_3 X^2 \pm k_4 XY + k_5 Y^2 \tag{5a}$$

$$0 = c_0 \pm c_1 Y + c_2 X - c_3 Y^2 \pm c_4 YX + c_5 X^2. \tag{5a}$$

In order to evaluate the stability of the equilibrium point we must evaluate the derivatives $(\partial\dot{X}/\partial X)_0$, $(\partial\dot{X}/\partial Y)_0$, $(\partial\dot{Y}/\partial X)_0$, and $(\partial\dot{Y}/\partial Y)_0$ at the steady state in order to set up the following 2×2 determinantal equation analogous to Eq. (2):

$$\begin{vmatrix} \left(\frac{\partial\dot{X}}{\partial X}\right)_0 - \lambda & \left(\frac{\partial\dot{X}}{\partial Y}\right)_0 \\ \left(\frac{\partial\dot{Y}}{\partial X}\right)_0 & \left(\frac{\partial\dot{Y}}{\partial Y}\right)_0 - \lambda \end{vmatrix} = 0. \tag{6}$$

Differentiating (4a) and (4b) we obtain the four derivatives

$$\partial\dot{X}/\partial X = \pm k_1 - 2k_3X \pm k_4Y \tag{7a}$$

$$\partial\dot{X}/\partial Y = k_2 \pm k_4X + 2k_5Y \tag{7b}$$

$$\partial\dot{Y}/\partial X = c_2 \pm c_4Y + 2c_5X \tag{7c}$$

$$\partial\dot{Y}/\partial Y = \pm c_1 - 2c_3Y \pm c_4X \tag{7d}$$

These derivatives (7a–7d) are evaluated at the steady states represented by Eqs. (5a) and (5b). The resulting values are then substituted into determinantal Eq. (6). Solution of the resulting quadratic equation for the eigenvalues λ provides information concerning the stability of the resulting equilibria based on the signs of the real parts of the eigenvalues.

4. Extension to Systems with Three Reference Reactants

Consider now a chemical system containing three reference reactants X, Y, and Z and only unimolecular and bimolecular reactions. The analogues to Eqs. (4a) and (4b) have ten terms as exemplified by the following equation for $\dot{X}$:

$$\dot{X} = k_0 \pm k_1X + k_2Y + k_3Z \pm k_4XY \pm k_5XZ + k_6YZ - k_7X^2 + k_8Y^2 + k_9Z^2. \tag{8}$$

In order to obtain the entries for the determinantal Eq. (2) (Section 2) nine partial derivatives with four terms each must be evaluated at the steady states as exemplified by the following equation for $\partial\dot{X}/\partial X$:

$$\partial\dot{X}/\partial X = \pm k_1 \pm k_4Y \pm k_5Z - 2k_7X. \tag{9}$$

By expansion of the determinant in Eq. (2) we obtain a cubic Eq. (3) (Sect. 2) where

$$A = 1 \tag{10a}$$

B = a sum of three different four-term polynomials = a twelve term polynomial (10b)

C = a sum of six different binary products of four-term polynomials = a 96-term polynomial ($96 = 6 \cdot 4^2$) (10c)

D = a sum of six different ternary products of four-term polynomials = a 384-term polynomial ($384 = 6 \cdot 4^3$) (10d)

Thus a general treatment of the three reference reactant system by the Tyson-Light method [19] results in a cubic equation (3) with $1+12+96+384=493$ terms. In this 493-term equation we must substitute the equilibrium values of X, Y, and Z and then solve for λ in order to determine the signs of the real parts of the roots. Clearly this method is intractable for a general treatment of the three reference reactant system analogous to the Tyson–Light treatment [19] of the two reference reactant system.

The method discussed in this paper for evaluating the qualitative dynamics of chemical systems by examination of the flow topology around their unstable equilibrium points in contrast to the Tyson–Light method [19] can be extended beyond systems with two reference reactants to systems with three and possibly even more reference reactants without running into analogous problems of intractability. Furthermore, restrictions to systems containing exclusively unimolecular and bimolecular reactions are no longer necessary. This paper discusses application of these methods to systems containing three reference reactants. Well characterized chemical systems which have been definitely shown to contain more than three reference reactants have not yet been found. Furthermore, this work shows that three reference reactants are sufficient to model the interesting types of exotic dynamics including periodic (limit cycle), biperiodic (toroidal), and non-periodic (chaotic) oscillations.

5. Influence Diagrams

In order to use switching circuit theory [20] to examine the flow topology around unstable equilibrium points, a graphical method is first required to represent relationships between the reference reactants. A directed graph [28, 29] with one vertex for each reference reactant is used for this purpose. An edge is directed from a vertex representing a given reference reactant to a vertex representing another reference reactant whose rate of change in concentration is affected by the first reference reactant. Such a directed edge is given a positive weight if the relationship is one of activation and a negative weight if the relationship is one of inhibition. If a given reference reactant has no effect on another given reference reactant, then the corresponding directed edge vanishes. For convenience such directed graphs will be called *influence diagrams.*

At this point it is necessary to distinguish between *simple* and *composite* chemical systems. The dynamics of a simple chemical system can be represented by a single influence diagram throughout the entire relevant region of concentration space. However, a composite chemical system requires more than one influence diagram to represent its dynamics in the relevant region of concentration space. This paper will consider simple chemical systems where a single influence diagram is sufficient for the analysis of their dynamics. All of the known types of exotic dynamics including periodic (limit cycle), biperiodic (toroidal), and non-periodic (chaotic) oscillations can be modelled by simple chemical systems containing three reference reactants. Furthermore, it is

desirable to understand first the fundamental dynamics of simple chemical systems before studying ways of piecing such simple chemical systems together to form composite chemical systems.

The construction of influence diagrams can be clarified by considering their relationship to the kinetic equations. Consider two reference reactants X and Y. If $(\partial \dot{Y}/\partial X) < 0$ then the influence diagram contains an edge directed from the X vertex to the Y vertex with a negative weight indicating that X inhibits Y. Conversely, if $(\partial \dot{Y}/\partial X) > 0$ then the influence diagram contains an edge directed from the X vertex to the Y vertex with a positive weight indicating that X activates Y. A simple chemical system is thus one where the derivatives of the type $(\partial \dot{Y}/\partial X)$ do not change sign in the relevant region of concentration space.

Now consider a chemical system containing n reference reactants. In order to keep the number of cases tractable, particularly for the three reference reactant systems treated in detail in this paper, ignore self-activation (e.g. X activates X) and self-inhibition (e.g. X inhibits X) since their effects can be considered later. The maximum number of directed edges in an influence diagram not including self-inhibition and self-activation is twice the number of edges in the corresponding complete graph K_n where a complete graph is defined as a set of n vertices with a single undirected edge between every possible pair of vertices [30]. Furthermore, each of these directed edges can independently be positive (i.e. X activates Y), negative (i.e. X inhibits Y), or can vanish completely (i.e. X does not affect Y). Thus for a system containing two reference reactants, the complete graph K_2 (a straight line segment) has one "edge", the influence diagrams have a maximum of two edges (one from X to Y and one from Y to X) and there are $3^2 = 9$ different possible influence diagrams. Figure 1 shows these nine possible influence diagrams for two reference reactant systems. Similarly for a system containing three reference reactants, the complete graph K_3 (a triangle) has three edges, the influence diagrams have a maximum of $2 \cdot 3 = 6$ edges, and there are $3^6 = 729$ possible influence diagrams.

I have found all 729 of these possible influence diagrams for three reference reactant systems but it would be of little value and a waste of space to depict them individually in this paper. Instead it is convenient to group them together in *classes* and *families*. A *class* of influence diagrams consists of all such diagrams that can be superimposed by a symmetry operation considering all vertices to be equivalent (i.e. temporarily ignoring for classification purposes, the obvious differences between the different reference reactants). In other words vertex labellings are ignored when influence diagrams are grouped into classes.

Thus for the nine influence diagrams in Fig. 1, the pairs B and D, C and E, and G and H are each superimposable by two-fold rotations so that the members of each pair belong to the same class. The nine influence diagrams for a two reference reactant system thus form six classes: A, $B+D$, $C+E$, F, $G+H$, and J. All influence diagrams of a given class represent systems exhibiting identical

qualitative dynamics. It is therefore necessary to determine the qualitative dynamics of only one influence diagram in each class in order to know the qualitative dynamics for each member of the class. A *family* of influence diagrams consists of all influence diagrams which become identical when the distinction between plus and minus signs is dropped. In other words edge labellings are ignored when classes are grouped into families. Thus for the nine influence diagrams in Fig. 1, there are the three families A, $B+C+D+E$, and $F+G+H+J$. A *circuit* in an influence diagram (which represents feedback) consists of a path which starts with a given vertex and follows various edges in the directions of their arrows until the original vertex is reached again. The *length* of a circuit is the number of edges that must be traversed from the original vertex until the original vertex is reached again. A *loop* in an influence diagram is a circuit of length 1 (i.e. consisting of an edge starting and finishing at the same vertex). Loops represent self-activation or self-inhibition. The *circuit structure* of an influence diagram is important for determining its feedback properties. All influence diagrams belonging to the same family have the same circuit structure. An *oscillatable* influence diagram has the following two properties which correspond to the need for a connected influence diagram with circuits containing all reference reactants:

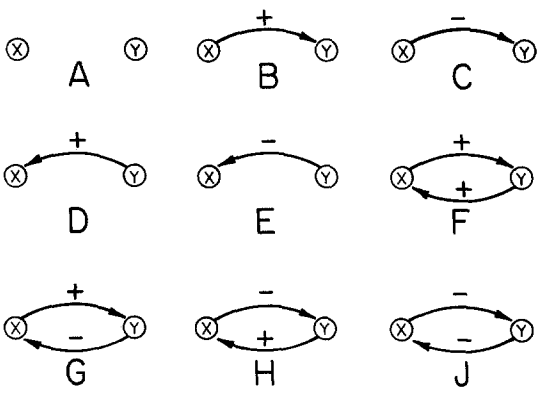

Fig. 1. The nine possible influence diagrams for systems containing two reference reactants X and Y excluding systems with loops (self-activation or self-inhibition)

1) Each vertex has at least one edge directed towards it (i.e., *a sink* in the graph theoretical sense [28, 29]) and one edge directed away from it (i.e., *a source* in the graph theoretical sense).

2) The directed graph representing the influence diagram is connected (i.e. consists of a single component so that every vertex can be reached from every other vertex by a path along the edges).

These two properties represent trivial necessary conditions for an influence diagram to represent an oscillatory process in which all of the state variables are reference reactants and are involved in the oscillation. For this reason we need to consider only such oscillatable influence diagrams when evaluating the dynamics of oscillating chemical systems.

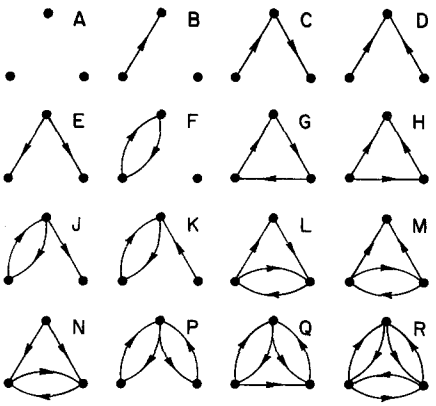

Fig. 2. The 16 families of possible influence diagrams for systems containing three reference reactants excluding systems with loops (self-activation or self-inhibition)

The 729 possible influence diagrams for three state variables can be divided into 16 families as depicted in Fig. 2. These families correspond to the digraphs with three points depicted by Harary [31]. Some of the important properties of these 16 families are summarized in Table 1. Only five of these 16 families containing a total of 416 possible influence diagrams are oscillatable and therefore can represent reference reactants in oscillating chemical systems.

6. Chemical Systems as Discrete Switching Networks

Consider a chemical system in which the concentrations of the reference reactants as defined above are the dependent variables and time is the

Table 1. Some properties of the 16 families of possible influence diagrams for systems with three reference reactants

Family (Fig. 2)	Number of classes	Total number of influence diagrams	Number of edges	Number of circuits	Connected	Oscillatable
A	1	1	0	0	No	No
B	2	12	1	0	No	No
C	4	24	2	0	Yes	No
D	3	12	2	0	Yes	No
E	3	12	2	0	Yes	No
F	3	12	2	1	No	No
G	4	16	3	1	Yes	Yes
H	8	48	3	0	Yes	No
J	8	48	3	1	Yes	No
K	8	48	3	1	Yes	No
L	16	96	4	2	Yes	Yes
M	10	48	4	1	Yes	No
N	10	48	4	1	Yes	No
P	10	48	4	2	Yes	Yes
Q	20	192	5	3	Yes	Yes
R	16	64	6	5	Yes	Yes
Total	126	729				

independent variable. Each of the reference reactants can be assigned a discrete value of 1 if the first time derivative of its concentration is positive (i.e. increasing concentration) and a discrete value of 0 if the first time derivative of its concentration is negative (i.e., decreasing concentration). A synchronous switching network is then set up in which time is quantized so that the signs of the first time derivatives of the concentrations of the reference reactants at time $t+1$ are determined by their signs at time t [21].

The switching state at any given time of such a chemical system containing n reference reactants can be represented by an n-vector of 1's and 0's corresponding to the signs of the first time derivatives of the concentrations of each of the n reference reactants. Such an n-vector is called a *state vector.* The total possible number of different such state vectors is 2^n. These state vectors may be represented by the 2^n vertices of an n-dimensional cube (or square when $n=2$). Furthermore, the possible transitions from states at synchronous time t to those at time $t+1$ may be represented by arrows directed along the edges of the n-cube. In this treatment the discrete time scale t is chosen so that it advances one unit each time a single component of the state vector changes. The resulting n-cube with directed edges is called a *state transition diagram.* It represents transitions around an equilibrium point or region corresponding to the center of the n-cube where all of the first time derivatives of the reference reactant concentrations are zero. The transitions represented by the state transition diagram are significant if the center of the diagram represents an unstable equilibrium point or region. In this case the transitions represented by the state transition diagrams define the fundamental topology of the flow in the neighborhood of the unstable equilibrium point.

7. Generation of State Transition Diagrams from Influence Diagrams

The influence diagrams represent the activation and inhibition relationships involving the reference reactants. The state transition diagrams depict the qualitative features of important kinetic behavior on the basis of the flow topologies around unstable equilibrium points or regions. This section discusses a convenient method developed by Glass [23] for deriving the state transition diagram corresponding to a given influence diagram. This provides a simple method for determining the important possibilities for the dynamics of a given system from its rate equations.

The first step of this method uses the influence diagram to generate a *truth table,* so called by analogy with Boolean logic [20]. In order to show how such a truth table is generated let us consider possible effects of one reference reactant X on a second reference reactant Y. If X activates Y as depicted by a positive arrow from X to Y in the influence diagram, then in the truth table the values for Y in each possible state vector at time $t+1$ will correspond to the values for X at time t. This relates to the fact that when X activates Y, an increase in the concentration of X (represented by 1) will eventually lead to an increase in the concentration of Y (also represented by 1) and vice versa.

However, if X inhibits Y as depected by a negative arrow from X to Y in the influence diagram, then in the truth table the values for Y at time $t+1$ will be opposite of the values for X at time t (i.e., a 0 for X at time t will lead to a 1 for Y at time $t+1$ and vice versa). This relates to the fact that when X inhibits Y, an increase in the concentration of X (represented by 1) will eventually lead to a decrease in the concentration of Y (represented by 0). These effects are summarized in Table 2.

Table 2. General effects of activation and inhibition on the truth table

Time t X	Time $t+1$ Y
0	0
1	1

X activates Y

$X \xrightarrow{+} Y$

Time t X	Time $t+1$ Y
0	1
1	0

X inhibits Y

$X \xrightarrow{-} Y$

Table 3 illustrates applications of this procedure for determination of the truth tables for the four oscillatable two reverence reactant systems F, G, H, and J in Fig. 1. Thus in the truth table for system F where X activates Y and Y activates X, the Y column for time $t+1$ is the same as the X column for time t and the X column for time $t+1$ is the same as the Y column for time t.

Table 3. Truth tables for oscillatable two reference reactant systems

Initial state time $= t$	State at time $= t+1$ F^a	G^a	H^a	J^a
X Y	X Y	X Y	X Y	X Y
0 0	0 0^{*d}	1 0^{**e}	0 1^{**e}	1 1
1 0	0 1	1 1^{**e}	0 0^{**e}	1 0^{*d}
0 1	1 0	0 0^{**e}	1 1^{**e}	0 1^{*d}
1 1	1 0	0 0^{**e}	1 1^{**e}	0 1^{*d}
Type of state transition diagram (Fig. 3)	B_2	C_2	C_2^b	B_2^c

[a] See Fig. 1.
[b] Direction reversed over C_2 in Fig. 3.
[c] B_2 in Fig. 3 rotated 90°.
[d] Attracting regions (i.e., steady time derivative polarity).
[e] Transitions involving change of only a single vector component.

There remains the problem of determining a state transition diagram for a given truth table. The following algorithm developed by Glass [23] can be used for this purpose:

1) Select two state vectors corresponding to an edge of the n-cube and the state of the system at time t. Such a pair of state vectors will be identical except for one component (conveniently called the *switching component*). In one of the state vectors chosen the switching component will be 0 corresponding to a negative first time derivative of the concentration of the corresponding reference reactant (conveniently called the *switching reference reactant*). In the other state vector chosen the switching component will be 1 corresponding to a positive time derivative of the switching reference reactant.

2) Compare the switching components in the corresponding state vectors at discrete time $t+1$. If both such components are 0, then the arrow on the corresponding edge of the n-cube will be directed towards the vertex corresponding to the state vector (at discrete time t) where the switching component is 0. If both components corresponding to the switching reference reactant for corresponding state vectors at discrete time $t+1$ are 1, then the arrow on the corresponding edge of the n-cube will be directed towards the vertex corresponding to the state vector (at discrete time t) where the switching component is 1. The third and remaining possibility, where one component corresponding to the switching reference reactant for the corresponding state vector at discrete time $t+1$ is 0 and the other such component is 1, prevents the assignment of an edge direction, but this possibility only arises when considering a feedback circuit not containing the switching reference reactant.

3) Repeat this procedure for the other pairs of state vectors corresponding to the remaining edges of the n-cube until all of the edges have been considered.

Let us now illustrate this procedure by converting the truth tables in Table 3 to the state transition diagrams in Fig. 3. Consider first the truth table for F in Fig. 1 given in Table 3. For the 00–10 edge the switching reference reactant is X and the switching component for both vectors at time $t+1$ is 0. Therefore the arrow on the 00–10 edge must point towards the 00 vertex. Similarly, for the 00–01 edge the switching reference reactant is Y and the switching component for both vectors at time $t+1$ is 0. Therefore, the arrow on the 00–01 edge must also point towards the 00 vertex. Similarly, the arrows on the 11–10 and the 11–01 edges both must point towards the 11 vertex since in both cases the switching component of the state vectors at time $t+1$ is 1. These four edge directions correspond to the B_2 state transition diagram of Fig. 3. The B_2 state transition diagram can represent a bistable system where the unstable equilibrium point is a saddle point on the energy surface between two attracting regions. The vertices 00 and 11 in the B_2 state transition diagram in Fig. 3 correspond to the attracting regions in this dynamic system. A characteristic feature of such attracting regions is that their state vectors do not change from time t to time $t+1$ on the discrete time scale.

Now let us consider the truth table for G in Fig. 1 given in Table 3. In this case the switching component of the 00–10 edge corresponding to the reference reactant X is 1 at time $t+1$ for both state vectors. Therefore, the arrow on the 00–10 edge must point towards the 10 vertex. Continuing the same procedure

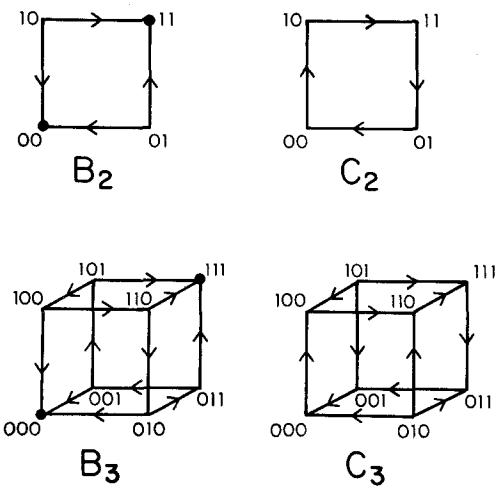

Fig. 3. State transition diagrams resulting from two and three reference reactant systems containing a single feedback circuit

for the remaining edges of the state transition square defines the directions of the edge arrows as 00→10, 10→11, 11→01, and 01→00, thereby leading to the C_2 state transition diagram of Fig. 3. This C_2 state transition diagram appears to be a necessary condition for a limit cycle surrounding the unstable equilibrium point.

Analogous procedures show that the influence diagram H in Fig. 1 leads to a C_2 state transition diagram with the limit cycle turning in the opposite direction to that given in Fig. 3. Similarly the influence diagram J in Fig. 1 leads to a B_2 state transition diagram rotated by 90° relative to that in Fig. 3 so that the 01 and 10 vertices rather than the 00 and 11 vertices correspond to the attracting regions. We thus see how all of the possible oscillatable two reference reactant systems lead either to bistable systems (B_2 in Fig. 3) or limit cycles (C_2 in Fig. 3). Indeed circuits of length 2 and types F and J in Fig. 1 will be classified as B_2 circuits and those of types G and H in Fig. 1 will be classified as C_2 circuits. This classification is useful when dissecting more complex chemical dynamic systems containing multiple feedback circuits.

Now let us consider oscillatable three reference reactant systems containing a single feedback circuit. These are four classes of possible influence diagrams corresponding to the four classes of family G in Fig. 2 (see Table 1). Prototypes of these four classes of possible influence diagrams are depicted in Fig. 4. The corresponding truth tables are depicted in Table 4. These lead to two basic types of state transition diagrams labelled as B_3 and C_3 in Fig. 3.

Consider first the influence diagram A in Fig. 4. The corresponding truth table (Table 4) shows that the state vectors 000 and 111 in the state transition diagram represent attracting regions. Application of the Glass algorithm outlined above shows that the three edges 100–000, 010–000, and 001–000 are all directed towards the 000 vertex and the three edges 110–111, 101–111, and 011–111 are all directed towards the 111 vertex. The remaining six edges of

Table 4. Truth tables for oscillatable three reference reactant systems with a single feedback circuit

Initial state time = t	State at time = $t+1$ of influence diagrams in Fig. 4											
	A			B			C			D		
X Y Z	X	Y	Z	X	Y	Z	X	Y	Z	X	Y	Z
0 0 0	0	0	0^a	1	0	0^b	1	0	1	1	1	1
1 0 0	0	1	0	1	1	0^b	1	1	1	1	0	1^b
0 1 0	0	0	1	1	0	1	1	0	0	1	1	0^b
0 0 1	1	0	0	0	0	0^b	0	0	1^a	0	1	1^b
1 1 0	0	1	1	1	1	1^b	1	1	0^a	1	0	0^b
1 0 1	1	1	0	0	1	0	0	1	1	0	0	1^b
0 1 1	1	0	1	0	0	1^b	0	0	0	0	1	0^b
1 1 1	1	1	1^a	0	1	1^b	0	1	0	0	0	0
Type of state transition diagram (*Fig.* 3)	B_3			C_3			B_3			C_3		

[a] Attracting regions: state vector remains unchanged.
[b] Transitions involving change of only a single vector component.

the state transition cube form a cycle but this is an antilimit cycle [32] rather than a limit cycle since a slight perturbation will cause this system to move towards one of the attracting regions 000 or 111. The resulting state transition diagram is B_3 in Fig. 3. The B_3 system can represent a bistable system with two attracting regions like the B_2 system discussed above. There are three other versions of the B_3 system which are equivalent to that depicted in Fig. 3 but which have 100 and 011, 101 and 010, and 110 and 001 as the pairs of attracting regions. These arise from the three equivalent influence diagrams of type C in Fig. 4 where unique positive arrow joins X to Y, Y to Z, or Z to X, respectively. Feedback circuits of the types A and C in Fig. 4 are therefore called B_3 circuits and in the absence of other circuits generate bistable systems around unstable equilibrium points (bifurcation points).

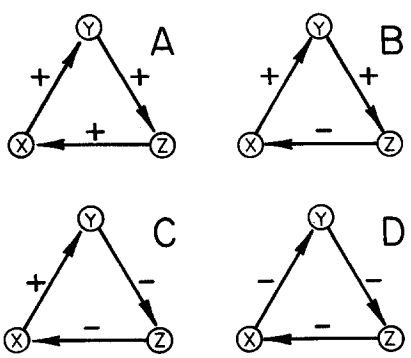

Fig. 4. Prototypes of the four classes of influence diagrams of the three reference reactant systems containing a single feedback circuit

Now let us consider the influence diagram B in Fig. 4. Application of the Glass algorithm to the corresponding truth table (Table 4) produces a state transition diagram with the following features:

1) The directions of the arrows on the six edges $000 \rightarrow 100$, $100 \rightarrow 110$, $110 \rightarrow 111$, $111 \rightarrow 011$, $011 \rightarrow 001$, and $001 \rightarrow 000$ define a cycle of length 6.

2) The remaining six edges are oriented towards this cycle so that it can function as a true limit cycle (in contrast to the cycle of length 6 in the B_3 system discussed above). It therefore is a *cyclic attractor* in the terminology of Glass and Pasternack [25].

3) The vertices 101 and 010 have all of their edges directed away from these vertices and therefore represent repelling regions.

This state transition diagram corresponds to C_3 in Fig. 3. This system corresponds to the dynamics of the Belousov–Zhabotinskii reaction [21]. There are three other symmetry-related versions of the C_3 state transition diagram (Fig. 3). The two with 100 and 011 and with 001 and 110 as the pairs of vertices representing repelling regions result from influence diagrams similar to B (Fig. 4) but with the unique negative edge joining X to Y and Y to Z, respectively. The third symmetry-related version of the C_3 state transition diagram has 000 and 111 as the pair of repelling regions and arises from the influence diagram D in Fig. 4. Furthermore, reversing the directions of the circuit in the influence diagrams B and D reverses the direction of the limit cycle in the corresponding state transition diagram.

There is an interesting duality of the partitioning of the eight vertices of the cubes in the B_3 and C_3 state transition diagrams. In the B_3 state transition diagram two vertices represent attracting regions and the remaining six vertices form a possible antilimit cycle (*or cyclic repeller*). Conversely, in the C_3 state transition diagram two vertices represent repelling regions and the remaining six vertices form a possible limit cycle (i.e., *cyclic attractor*).

8. Three Reference Reactant Systems Containing Multiple Feedback Circuits

The previous sections show that simple chemical systems containing two or three reference reactants and a single feedback circuit generate two competing attracting regions (e.g., B_2 and B_3 in Fig. 3) or limit cycles (e.g., C_2 and C_3 in Fig. 3) around unstable equilibrium points. We now wish to consider possible three reference reactant systems containing two feedback circuits of the following types:

1) Systems containing one circuit of length 3 and one circuit of length 2 (i.e., B_2+B_3, C_2+B_3, B_2+C_3, and C_2+C_3).

2) Systems containing two circuits of lengths 2 (i.e., B_2+B_2, B_2+C_2, and C_2+C_2).

The influence diagrams for possible systems containing one circuit of length 2

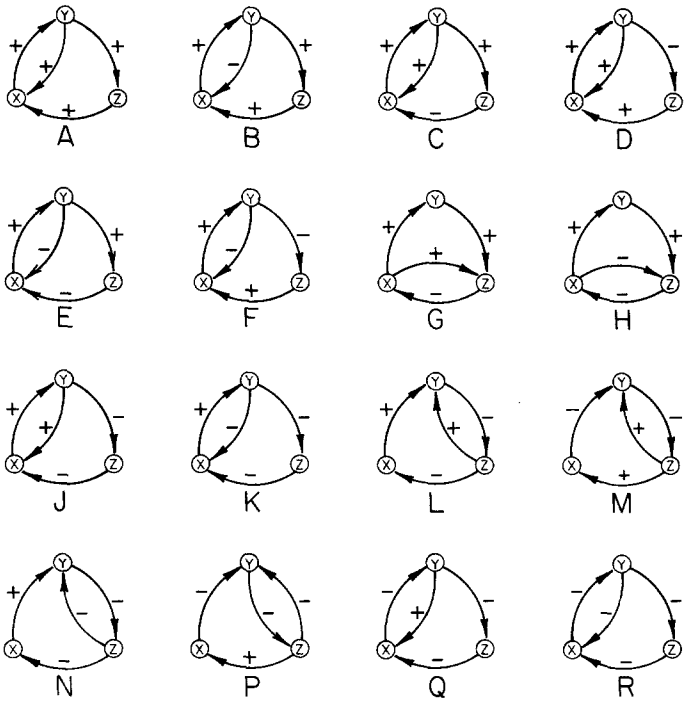

Fig. 5. Influence diagrams for 16 classes of three reference reactant systems containing one feedback circuit of length 3 and one feedback circuit of length 2

and one circuit of length 3 are illustrated in Fig. 5. Similarly, the influence diagrams of possible systems containing two circuits of length 2 are depicted in Fig. 6. In Figs. 5 and 6 only one influence diagram of each of the possible classes is depicted. The corresponding truth tables are given in Tables 5 and 6. Examples of state transition diagrams for the seven possible binary superpositions of B_2, B_3, C_2, and C_3 circuits are depicted in Fig. 7. These were determined from the truth tables (Tables 5 and 6) by the Glass algorithm with the following additional features:

1) The effects of each feedback circuit must be considered separately. Thus any edge arrow direction possible for an individual feedback circuit must also be considered possible for a multiple feedback circuit system containing this particular individual feedback circuit.

2) In some cases, consideration of the different feedback circuits will lead to opposing arrow directions on a given edge of the n-cube. In such cases movement along this edge in both directions is possible.

3) Addition of feedback circuits will increase the freedom of motion along the edges of the n-cube thereby increasing the number of cycles and removing attracting regions.

4) The effects of superposing the basic types of individual feedback circuits B_2,

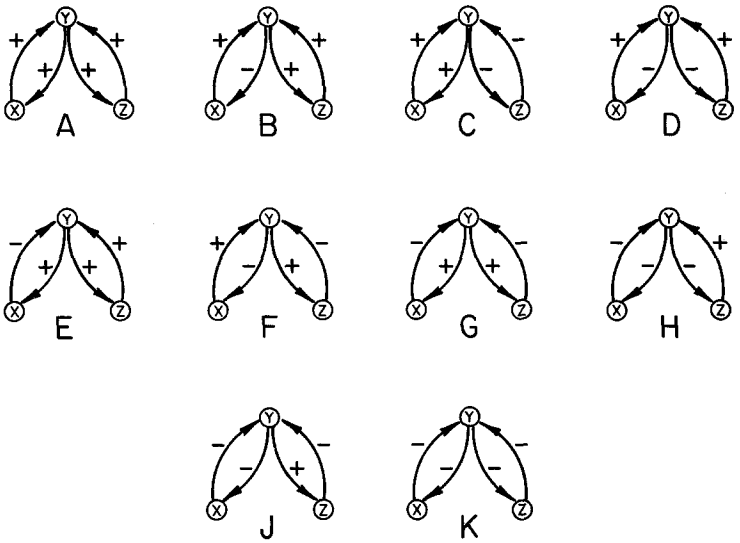

Fig. 6. Influence diagrams for 10 classes of three reference reactant systems containing two feedback circuits of length 2

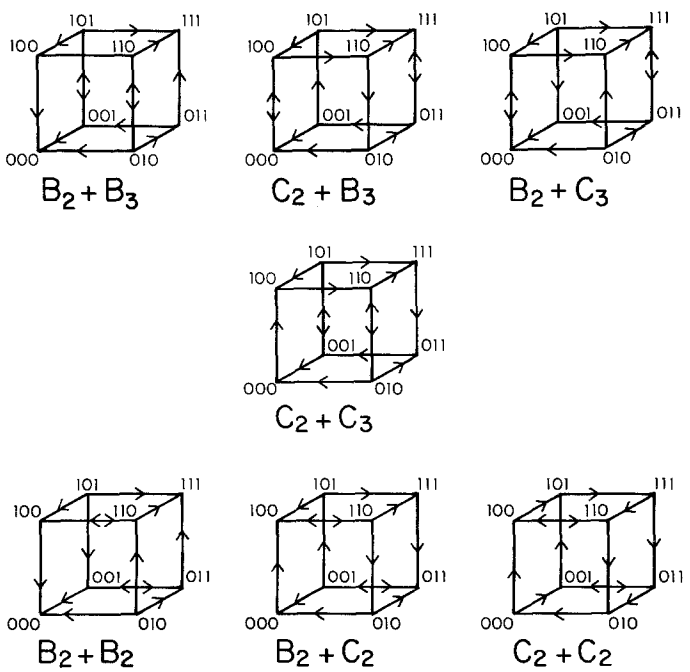

Fig. 7. Examples of state transition diagrams for three reference reactant systems containing two feedback circuits

Table 5. Truth tables for representative three reference reactant systems with two circuits: one of length 3 and one of length 2

Initial state time = t	State at time = $t+1$ B_3+B_3 (A in Fig. 5)		C_2+B_3 (B in Fig. 5)		B_2+C_3 (C in Fig. 5)		C_2+C_3 (E in Fig. 5)	
	2 circuit	3 circuit	2 circuit	3 circuit	2 circuit	3 circuit	2 circuit	3 circuit
$X\ Y\ Z$	$X\ Y\ Z$	$X\ Y\ Z$	$X\ Y\ Z$	$X\ Y\ Z$	$X\ Y\ Z$	$X\ Y\ Z$	$X\ Y\ Z$	$X\ Y\ Z$
0 0 0	0 0 0^a	0 0 0^a	1 0 0^b	0 0 0^a	0 0 0^a	1 0 0^b	1 0 0^b	1 0 0^b
1 0 0	0 1 0	0 1 0	1 1 0^b	0 1 0	0 1 0	1 1 0^b	1 1 0^b	1 1 0^b
0 1 0	1 0 0	0 0 1	0 0 0^b	0 0 1	1 0 0	1 0 1	0 0 0^b	1 0 1
0 0 1	0 0 1^a	1 0 0	1 0 1	1 0 0	0 0 1^a	0 0 0^b	1 0 1^b	0 0 0^b
1 1 0	1 1 0^a	0 1 1	0 1 0^b	0 1 1	1 1 0^a	1 1 1^b	0 1 0^b	1 1 1^b
1 0 1	0 1 1	1 1 0	1 1 1^b	1 1 0	0 1 1	0 1 0	0 0 1^b	0 1 0
0 1 1	1 0 1	1 0 1	0 0 1^b	1 0 1	1 0 1	0 0 1^b	0 0 1^b	0 0 1^b
1 1 1	1 1 1^a	1 1 1^a	0 1 1^b	1 1 1^a	1 1 1^a	0 1 1^b	0 1 1^b	0 1 1^b

[a] Transitions involving an unchanged state vector.
[b] Transitions involving change of only a single vector component.

Table 6. Truth tables for representative three reference reactant systems with two circuits of length 2

Initial state time = t	State at time = $t+1$ B_2+B_2 (A in Fig. 6)		B_2+C_2 (B in Fig. 6)		C_2+C_2 (D in Fig. 6)	
	Left circuit	Right circuit	Left circuit	Right circuit	Left circuit	Right circuit
$X\ Y\ Z$	$X\ Y\ Z$	$X\ Y\ Z$	$X\ Y\ Z$	$X\ Y\ Z$	$X\ Y\ Z$	$X\ Y\ Z$
0 0 0	0 0 0^a	0 0 0^a	1 0 0^b	0 0 0^a	1 0 0^b	0 0 1^b
1 0 0	0 1 0	1 0 0^a	1 1 0^b	1 0 0^a	1 1 0^b	1 0 1^b
0 1 0	1 0 0	0 0 1	0 0 0^b	0 0 1	0 0 0^b	0 0 0^b
0 0 1	0 0 1^a	0 1 0	1 0 1^b	0 1 0	1 0 1^b	0 1 1^b
1 1 0	1 1 0^a	1 0 1	0 1 0^b	1 0 1	0 1 0^b	1 0 0^b
1 0 1	0 1 1	1 1 0	1 1 1^b	1 1 0	1 1 1^b	1 1 1^b
0 1 1	1 0 1	0 1 1^a	0 0 1^b	0 1 1^a	0 0 1^b	0 1 0^b
1 1 1	1 1 1^a	1 1 1^a	0 1 1^b	1 1 1^a	0 1 1^b	1 1 0^b

[a] Transitions involving an unchanged state cector.
[b] Transitions involving change of only a single vector component.

B_3, C_2 and C_3 lead to consistent results regardless of the actual influence diagrams. More specifically, evaluating each of the possible binary superpositions once is sufficient to determine the correct dynamics for that particular binary superposition any time that it is encountered.

The state transition diagrams obtained from three reference reactant systems with two feedback circuits all correspond to one of the following three dynamic types:

1) Systems containing no cycles other than possibly a cyclic repeller leading into attracting regions. The B_2+B_3 (A, J, N, and P in Fig. 5) and B_2+B_2 (A,

C, and K in Fig. 6) systems are of this type. These systems like the equivalent B_3 system can represent a bistable system containing two attracting regions. Schematically we can say $B_3 = B_2 + B_3 = B_2 + B_2$.

2) Systems containing a single cyclic attractor: The $B_2 + C_3$ system (C, D, H, and R in Fig. 5) is of this type. This system like the equivalent C_3 system can represent a limit cycle oscillation. Schematically we can say $C_3 = B_2 + C_3$.

3) Systems containing several interlocking cycles: Such systems have one cycle of length 6 interlocked with two cycles of length 4 on opposite faces of the state transition cube. The $C_2 + B_3$ (B and K in Fig. 5), $C_2 + C_3$ (E, F, G, M, and Q in Fig. 5), $B_2 + C_2$ (B, E, H, and J in Fig. 6), and $C_2 + C_2$ (D, F, and G in Fig. 6) systems are all of this type. Such systems can represent toroidal (biperiodic) or chaotic (aperiodic) oscillations depending upon the synchronization between the cycles of different lengths. A minimum of two feedback circuits appears necessary for this type of dynamic behavior.

The state transition diagrams have also been checked for several of the possible systems of family Q in Fig. 2 which contains three feedback circuits: two of length 2 and one of length 3. However, addition of a third feedback circuit generates no new topological possibilities in state transition diagrams for the following reasons:

1) Adding a B_2 circuit does nothing: we have already seen how $B_2 + B_3 = B_3$ and $B_2 + C_3 = C_3$. The attracting regions of the B_2 circuit are destroyed by the other circuits so that the B_2 circuit has no effect on the dynamics.

2) If a B_2 circuit is absent, then a three-reference reactant system containing three or more feedback circuits must contain two C_2 circuits. However, the $C_2 + C_2$ combination is sufficient to generate interlocking cycles (chaotic topology) in the state transition diagram. Additional feedback circuits can only generate additional edges with arrows in both directions which at most will increase the number of interlocking cycles but with no fundamental changes in the underlying topology of the already chaotic system.

3) Self-activation and self-inhibition (positive and negative loops, respectively, in the influence diagram) do not affect the cycle structure of the state transition diagram since they only involve a single reference reactant (this can be verified by applying the Glass algorithm to actual cases containing self-activation and self-inhibition). However, as will be seen in the next section, self-activation and self-inhibition may have a major effect on the stability of equilibrium points.

9. The Existence of Unstable Equilibrium Points

The preceding sections have derived possible flow topologies around unstable equilibrium points in simple two and three reference reactant systems. Another requirement for realization of the corresponding dynamics in such systems is the existence of an unstable equilibrium point or region. An example of an unstable one-dimensional equilibrium region is an antilimit cycle [32]. In

systems containing two reference reactants evaluation of the stability of equilibrium points requires solution of the following determinental equation where the zero subscripts refer to the equilibrium point being evaluated:

$$\begin{vmatrix} \left(\frac{\partial \dot{X}}{\partial X}\right)_0 - \lambda & \left(\frac{\partial \dot{X}}{\partial Y}\right)_0 \\ \left(\frac{\partial \dot{Y}}{\partial X}\right)_0 & \left(\frac{\partial \dot{Y}}{\partial Y}\right)_0 - \lambda \end{vmatrix} = 0. \tag{6}$$

The equilibrium point is unstable if Eq. 6 has at least one root with a positive real part.

We have shown how solutions of equations corresponding to 6 rapidly become intractable in systems containing three or more reference reactants if the exact values of the required derivatives must be calculated. Thus in the case of the three reference reactant system expansion of a determinantal equation analogous to 6 (Eq. (2) in Sect. 2) to give the corresponding cubic characteristic equation (Eq. (3) in Sect. 2) involves a 493-term equation at one point. However, since a stability analysis requires only the *signs* of the real parts of the roots λ of the characteristic equations rather than the roots themselves, crude approximations can be used for the required derivatives $(\partial \dot{X}/\partial X)_0$, etc., without affecting the essential results of the stability analysis except in certain special cases discussed below. We therefore approximate the derivatives required for Eq. (6) in the following manner:

$$\left(\frac{\partial \dot{X}}{\partial X}\right)_0, \left(\frac{\partial \dot{X}}{\partial Y}\right)_0, \left(\frac{\partial \dot{Y}}{\partial X}\right)_0, \left(\frac{\partial \dot{Y}}{\partial Y}\right)_0 = \begin{cases} +1 \text{ if the actual derivative is positive} \\ 0 \text{ if the actual derivative is zero} \\ -1 \text{ if the actual derivative is negative.} \end{cases} \tag{12}$$

The process represented by Eq. (12) corresponds to determining the *adjacency matrix* [33] of the corresponding influence diagram. Solving Eq. (6) for the two reference reactant system and Eq. (2) for the three reference reactant system using the values of +1, 0, and −1 for the actual derivatives in accord with Eq. (12) corresponds to solving the characteristic equation [33] of this adjacency matrix for its eigenvalues. We now assume that the signs of the real parts of the eigenvalues obtained by this method will be the same as those which would arise if the actual values of the required partial derivatives $(\partial \dot{X}/\partial X)_0$, etc., were used. Close inspection of the actual characteristic equations obtained suggests the validity of this assumption is systems containing two or three reference reactants except for the $B_2 + C_2$ case discussed below. A rigorous proof of this point even for the three reference reactant systems would require a more detailed analysis of the root structure of the possible characteristic equations than is appropriate for this paper. However, this method is related to previously used methods for classifying instabilities in chemical reaction systems [34] and ecological networks [35].

The following results are obtained when this method is used for the stability analysis of simple two reference reactant systems without any loops:

1) The B_2 system (e.g., F in Fig. 1): The characteristic equation is λ^2-1 leading to the two roots ± 1. Since one of these has a positive real part (namely $+1$), this system has an unstable equilibrium point. Furthermore, the opposite signs of the real parts of the two roots suggest realizability of the bifurcation (saddle point) dynamics indicated by the B_2 state transition diagram.

2) The C_2 system (e.g., G in Fig. 1): The characteristic equation is λ^2+1 leading to the two roots $\pm i$ where $i=\sqrt{-1}$. Both of these roots have zero real parts. This suggests that the necessary unstable equilibrium point for true limit cycle oscillations cannot exist in a pure C_2 system in accord with the results of Tyson and Light [17].

The other variants of the B_2 and C_2 systems lead to the same characteristic equations. More generally, any influence diagrams belonging to the same *family* and exhibiting the same flow topology around unstable equilibrium points as determined by their state transition diagrams also lead to the same characteristic equation of their adjacency matrices. However, influence diagrams belonging to different families have different characteristic equations of their adjacency matrices even though their state transition diagrams may exhibit the same topology around unstable equilibrium points. Thus, the "equality" noted above $B_2,+B_3=B_2+B_2=B_3$ is valid when considering the flow topology around unstable equilibrium points but is not valid when considering the resulting characteristic equation in the stability analysis.

Tyson and Light [19] have indicated that adding a termolecular step of the type $2X+Y=3X$ can convert a two reference reactant system with the influence diagram G in Fig. 1 and C_2 topology but without the unstable equilibria required for limit cycle oscillations (i.e., only zero real parts of the roots of the characteristic equation) into another two reference reactant system which has an unstable equilibrium point and which therefore can exhibit limit cycle oscillations. This termolecular mechanism is well known [36, 37, 38] as the "Brusselator". However, the termolecular step $2X+Y=3X$ corresponds to adding self-activating properties for X. The resulting new positive loop converts the influence diagram G in Fig. 1 to the following influence diagram:

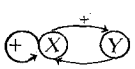

The characteristic equation of this influence diagram is $\lambda^2-\lambda+1=0$ with the roots $\frac{1}{2}(1\pm i\sqrt{3})$. The real parts of these roots are now positive (1/2) indicating the presence of an unstable equilibrium point. The cycle in the B_2 state transition diagram now becomes a limit cycle in accord with the established properties of the Brusselator [36, 37, 38]. This simple example also shows how addition of self-activation can make an equilibrium point unstable without affecting the flow topology around equilibrium points.

Now let us consider the two fundamentally different types of dynamic systems containing three reference reactants and a single feedback circuit. We arrive at the following characteristic equations with the indicated roots:

1) *The B_3 system* (*e.g., A in Fig.* 4): The characteristic equation is $\lambda^3-1=0$ which has one real root (+1) and two complex roots with $-1/2$ real parts.

2) *The C_3 system* (*e.g., B in Fig.* 4): The characteristic equation is $\lambda^3+1=0$ which has one real root (−1) and two complex roots with 1/2 real parts.

Similarly, the following characteristic equations with the indicated roots can be obtained for the dynamic systems containing three reference reactants and two feedback circuits, one of length 3 and one of length 2:

1) *The B_2+B_3 system* (*e.g., A in Fig.* 5): The characteristic equation is $\lambda^3-\lambda-1=0$ which has one real root (+1.32646) and two complex roots with −0.66323 real parts.

2) *The C_2+B_3 system* (*e.g., B in Fig.* 5): The characteristic equation is $\lambda^3+\lambda-1=0$ which has one real root (+0.68233) and two complex roots with −0.34116 real parts.

3) *The B_2+C_3 system* (*e.g., C in Fig.* 5): The characteristic equation is $\lambda^3-\lambda+1=0$ which has one real root (−0.68233) and two complex roots with +0.34116 real parts.

4) *The C_2+C_3 system* (*e.g., E in Fig.* 5); The characteristic equation is $\lambda^3+\lambda+1=0$ which has one real root (−1.32646) and two complex roots with +0.66323 real parts.

All other influence diagrams in Figs. 4 and 5 generate identical characteristic equations to those listed above for the influence diagram leading to the same topology around the unstable equilibrium point.

The important thing to note from these characteristic equations of three reference reactant systems containing a circuit of length three is that all of them have at least one root with a positive real part. This means that all of these systems can have the unstable equilibrium points required for the types of dynamic behavior indicated by their state transition diagrams. The relationship of this to elementary principles in algebraic graph theory [33] is outlined in Appendix 1.

Somewhat different results are obtained in the cases of the systems containing three reference reactants and two feedback circuits of length two (e.g., those of family *P* in Fig. 2). For such systems the following characteristic equations with the indicated roots are obtained:

1) *The B_2+B_2 system* (*e.g., A in Fig.* 6): The characteristic equation is $\lambda^3-2\lambda=0$ which has the roots 0, $\sqrt{2}$, and $-\sqrt{2}$.

2) *The B_2+C_2 system* (*e.g., B in Fig.* 6): The characteristic equation is $\lambda^3=0$ which has three zero roots.

3) *The C_2+C_2 system* (*e.g., D in Fig.* 6): The characteristic equation is $\lambda^3+2\lambda=0$ which has the roots 0, $i\sqrt{2}$, and $-i\sqrt{2}$.

All of these systems have characteristic equations with one zero root and two roots of equal absolute value and opposite signs. These last two roots may either have a real component or be pure imaginary. If they are pure imaginary (e.g., the C_2+C_2 system) then an unstable equilibrium point is absent. The system therefore cannot have the unstable equilibrium point required for realization of the dynamics indicated by the state transition diagram. The B_2+C_2 system, which generates a characteristic equation with all roots zero, is a borderline case between the B_2+B_2 system with an unstable equilibrium point (i.e., the positive $\sqrt{2}$ root) and the C_2+C_2 system without an unstable equilibrium point. For this reason, the presence of an unstable equilibrium point in the B_2+C_2 system will be sensitive to the relative values of the various rate constants. A more precise treatment considering the actual values of the rate constants is necessary in order to determine the presence or absence of unstable equilibrium points in the B_2+C_2 system, whereas the simplified treatment used in this section appears sufficient to determine the presence or absence of unstable equilibrium points in all of the other systems.

The general pattern emerging from the treatment in this section is that systems containing feedback circuits of length three always have unstable equilibrium points whereas systems containing only feedback circuits of length two, particularly those containing cycles in their state transition diagrams such as C_2 and C_2+C_2, may not have unstable equilibrium points. However, addition of self-activation (a positive loop) to a system containing only feedback circuits of length two (to give, for example, a B_1+C_2 system) can generate an unstable equilibrium point.

10. Relationship to Known Systems Exhibiting Chaos and Toroidal Oscillations

We now extend the treatment discussed in the previous sections to some dynamic systems reported by previous workers to exhibit chaos (nonperiodic oscillation) or toroidal (biperiodic) oscillation. In all cases these systems are composite systems which require two influence diagrams to represent the entire relevant region of concentration space. However, since in all cases both of the influence diagrams of the composite system lead to similar dynamics, this complication is not serious. Fig. 8 shows some influence diagrams pertaining to several such systems containing three reference reactants.

Consider first the Lorenz equations reported [12, 39] to exhibit continuous chaos:

$$\dot{X} = -10X + 10Y \tag{13a}$$

$$\dot{Y} = 28X - Y - XZ \tag{13b}$$

$$\dot{Z} = XY - (8/3)Z \tag{13c}$$

The influence diagram of this system will depend on whether Z is greater or less than 28. If $Z<28$ the influence diagram is A in Fig. 8. Ignoring the three self-inhibition loops this is a $B_2+C_2+C_3=C_2+C_3$ system. If $Z>28$ we get an

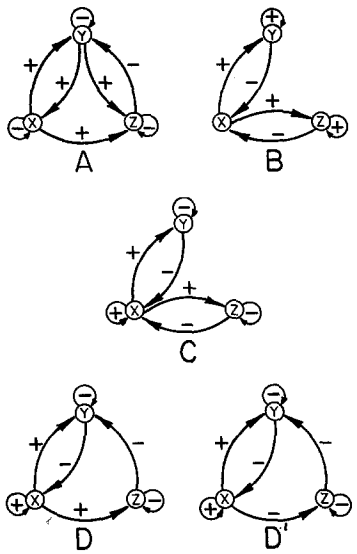

Fig. 8. Influence diagrams of dynamic systems reported to exhibit chaos or toroidal oscillation

influence diagram corresponding to a $C_2+C_2+C_3$ system. Both of these systems contain the interlocking cycles required for chaos.

Rössler has modified the Lorenz equations (13a)–(13c) to give the following system [12] exhibiting a chaotic flow:

$$\dot{X} = -Y - Z \tag{14a}$$

$$\dot{Y} = X + 0.2Y \tag{14b}$$

$$\dot{Z} = 0.2 + XZ - 5.7Z \tag{14c}$$

If $X > 5.7$ the influence diagram of this system is B in Fig. 8. If $X < 5.7$ the influence diagram is identical to B in Fig. 8 except for a change in the sign of the loop on Z from positive to negative. Another one of Rössler's systems exhibiting chaotic flow is the following:

$$\dot{X} = X - XY - Z \tag{15a}$$

$$\dot{Y} = X^2 - aY \tag{15b}$$

$$\dot{Z} = bX - cZ + d. \tag{15c}$$

If $Y < 1$ the influence diagram of this system is C in Fig. 8. If $Y > 1$ the influence diagram is identical to C in Fig. 8 except for a change in the sign of the loop on X from positive to negative. We therefore see that both (14a)–14c) and (15a)–(15c) are composite systems which have identical influence diagrams if self-activation and self-inhibition loops are ignored. Both are C_2+C_2 systems. We have shown above how the C_2+C_2 system gives a state transition diagram containing the interlocking cycles required for chaotic oscillations around unstable equilibrium points but does not generate an unstable equilibrium point. However, addition of self-activation loops to a C_2+C_2 system can convert existing equilibrium points into unstable ones as was shown above for the simpler C_2 system.

Rössler has used the following system of equations for generating toroidal oscillations [11]:

$$\dot{X} = aX - Y\left(\frac{X}{X+k_1}\right) + c \tag{16a}$$

$$\dot{Y} = X - bY - Z\left(\frac{Y}{Y+k_2}\right) \tag{16b}$$

$$\dot{Z} = \mathrm{d}X - e(X^2 - f)\left(\frac{Z}{Z+k_3}\right). \tag{16c}$$

In this case the influence diagram depends on whether the term $\mathrm{d}X$ or the term $-eX^2\left(\frac{Z}{Z+k_3}\right)$ dominates in the expression for $\dot{Z}$. If the term $\mathrm{d}X$ dominates, then the influence diagram for system (16a)–(16c) is D in Fig. 8. Ignoring the circuits of length 1, this is a C_2+B_3 system. If the term $-eX^2\left(\frac{Z}{Z+k_3}\right)$ dominates, then the influence diagram for system (16a)–(16c) is D' in Fig. 8. Ignoring the circuits of length 1, this is a C_2+C_3 system. Both the C_2+C_3 and the C_2+B_3 systems (Fig. 7) contain the interlocking cycles required for chaotic or toroidal oscillations. Differentiation between chaotic and toroidal oscillations requires a more precise calculation on this specific system and thus is beyond the scope of the methods used in this paper. In any case, however, the techniques outlined in this paper clearly indicate that Rössler's systems represented by Eqs. (16a)–(16c) have state transition diagrams containing the interlocking cycles required for toroidal oscillations and thus are consistent with his observations.

A further observation is the presence of loops, including particularly negative loops representing self-inhibition, in the known systems exhibiting chaotic oscillations in addition to appropriate combinations of circuits of lengths two and three to account for the observed qualitative dynamics. The analysis in this paper indicates that the loops in the influence diagrams corresponding to Eqs. (13a)–(13c), (14a)–(14c), (15a)–(15c), and (16a)–(16c) are not necessary to generate the correct topology around the unstable equilibrium points. However, one self-activation loop is needed in the two systems (14a)–(14c) and (15a)–(15c) to generate an unstable equilibrium point in the C_2+C_2 system, which otherwise would not have the unstable equilibrium point required for realization of the dynamics indicated by its state transition diagram. The self-inhibition loops are probably needed in order to prevent an unbounded increase in the concentrations of the reference reactants. However, it nevertheless might be possible to find systems exhibiting toroidal oscillations and chaos containing fewer self-activation and self-inhibition loops but with otherwise similar influence diagrams to those depicted in Fig. 8.

11. Conclusions

This paper shows that the following four-step procedure is useful for investigating the qualitative dynamics of simple chemical systems containing three and possibly even more reference reactants: 1) An influence diagram is constructed representing the relationships between the reference reactants; 2) This influence diagram is used to generate a truth table indicating possible transitions between state vectors representing the signs of the time derivatives of the reference reactant concentrations; 3) The resulting truth table is used to determine a state transition diagram representing the flow topology of unstable equilibrium points as directed edges of a cube; 4) The characteristic equation of the adjacency matrix of the influence diagram is solved to determine the possible presence of an unstable equilibrium point associated with realization of the dynamics indicated by the state transition diagram.

This method has been applied to all possible dynamic systems containing two or three reference reactants with the minimally necessary activation-inhibition relationships for oscillatory behavior. In the case of systems containing two reference reactants, there are only two basic types of dynamic behavior corresponding to bistable systems (B_2) and limit cycles (C_2). However, the C_2 system requires an additional self-activation loop to acquire the unstable equilibrium point associated with realization of limit cycle oscillations. Adding a third reference reactant generates the additional possibility of systems containing interlocking cycles (e.g., C_2+B_3) which can correspond to systems exhibiting chaos or toroidal oscillations.

The challenge to the chemist lies in finding real chemical systems exhibiting these various types of exotic dynamic behavior. Several examples are known of real chemical systems exhibiting limit cycle oscillations (e.g., the Belousov–Zhabotinskii and the Bray–Liebhafsky reactions). However, real chemical systems have not yet been found exhibiting some of the more exotic of the above types of dynamic behavior including toroidal (biperiodic) oscillations and chaos (aperiodic oscillations). The treatment in this paper shows how realization of these more unusual types of kinetics requires the discovery or design of real chemical systems containing two or more interlocking feedback circuits of the correct types.

Acknowledgments. I am pleased to acknowledge helpful discussions with Prof. John Garst (Department of Chemistry, University of Georgia) and useful comments by Prof. Frank Harary (Department of Mathematics, University of Michigan). In addition, detailed comments by Prof. Leon Glass (Department of Physiology, McGill University) on an earlier version of this paper were extremely helpful in writing the final version.

Appendix

The Appendix outlines a proof for the following lemma which arises during the course of the treatment of this paper:

Lemma: A dynamic system represented by an influence diagram containing three vertices, a circuit of length 3, and no loops (i.e., no self-activation or self-inhibition) must have an unstable equilibrium point.

Proof: A dynamic system represented by such a graph has an unstable equilibrium point if the cubic equation derived from the expansion of the determinant of its adjacency matrix (see Eq. (2) in the text)

$$A\lambda^3 + B\lambda^2 + C\lambda + D = 0 \tag{3}$$

has at least one root with a positive real part [26, 27]. The coefficients in Eq. (3) have the following significance in terms of the expansion of the determinant of the adjacency matrix in terms of sesquivalent subgraphs [40, 41]:

$$A = 1 \tag{17a}$$

$$B = \text{the sum of the weights of the loops} \tag{17b}$$

$$C = \text{the sum of the weights of circuits of length 2} \tag{17c}$$

$$D = \text{the sum of the weights of circuits of length 3.} \tag{17d}$$

The weight of a circuit (e.g., (17c) and (17d)) is determined by multiplying the weights of all of the directed edges forming the circuit.

The assumption of the absence of loops in the influence diagram means that B must be zero. Furthermore the assumption that there is a circuit of length 3 means that D cannot be zero. Eq. (3) therefore becomes Eq. (18) where C can be any positive or

$$\lambda^3 + C\lambda + D = 0 \tag{18}$$

negative real number including zero.

Inspection of the standard formulas for the roots of cubic equations [42] reveals that the sums of the real parts of the three roots of an equation of the form (18) (i.e., one with no λ^2 term) must be zero. This means that Eq. (18) must have at least one root with a positive real part unless all three roots are zero or pure imaginary (i.e., zero real part). However, the product of the three roots must be $D \neq 0$. Therefore none of the roots of Eq. (18) ($D \neq 0$) can be zero, at least two of the three roots must have non-zero real parts, and at least one of these non-zero real parts must be positive. Therefore, a dynamic system represented by a graph with a characteristic Eq. (18) ($D \neq 0$) corresponding to the presence of a circuit of length 3 must have an unstable equilibrium point.

References

1. For part 7 of this series see: King, R. B., Rouvray, D. H.: J. Am. Chem. Soc. **99,** 7834 (1977)
2. Bray, W. C.: J. Am. Chem. Soc. **43,** 1262 (1921)
3. Bray, W. C., Liebhafsky, H. A.: J. Am. Chem. Soc. **53,** 38 (1931)
4. Belousov, B.: Sb. Ref. Rad. Med. 145, (1958)
5. Zhabotinskii, A. M.: Biofizika **9,** 306 (1964)
6. Zhabotinskii, A. M.: Dokl. Akad. Nauk SSSR **157,** 392 (1964)

7. Nicolis, G., Portnow, J.: Chem. Rev. **73,** 365 (1973)
8. Noyes, R. M., Field, R. J.: Ann. Rev. Phys. Chem. **25,** 95 (1974)
9. Frank, U. F.: Angew. Chem. Int. Ed. **17,** 1 (1978)
10. Murray, J. D.: Lectures on nonlinear differential equation models in biology. Oxford: Clarendon Press 1977
11. Rössler, O. E.: Z. Naturforsch. **32a,** 299 (1977)
12. Rössler, O. E.: Phys. Lett. **57A,** 397 (1976)
13. Rössler, O. E.: Z. Naturforsch. **31a,** 1664 (1976)
14. Rössler, Z. Naturforsch. **31a,** 1168 (1976)
15. Noyes, R. M., Field, R. J., Körös, E.: J. Am. Chem. Soc. **94,** 1394 (1972)
16. Field, R. J., Körös, E., Noyes, R. M.: J. Am. Chem. Soc. **94,** 8649 (1972)
17. Sharma, K. R., Noyes, R. M.: J. Am. Chem. Soc. **98,** 4345 (1976)
18. Higgins, J.: Ind. and Eng. Chem. **59,** 18 (1967)
19. Tyson, J. J., Light, J. C.: J. Chem. Phys. **59,** 4164 (1973)
20. Caldwell, S. H.: Switching circuits and logical design. New York: Wiley 1958, 1967
21. Glass, L.: J. Theor. Biol. **54,** 85 (1975)
22. Glass, L.: J. Chem. Phys. **63,** 1325 (1975)
23. Glass, L., in: Statistical mechanics, Pt. B, Berne, B. J., Ed. New York: Plenum Press 1977
24. Glass, L., Pasternack, J. S.: Bull. Math. Biol. **40,** 27 (1978)
25. Glass, L., Pasternack, J. S.: J. Math. Biol. **6,** 207 (1978)
26. Hirsch, M. W., Smale, S.: Differential equations, dynamical systems, and linear algebra, Chap. 9. New York: Academic Press 1974
27. Hirsch, M. W., Smale, S.: Differential equations, dynamical systems, and linear algebra, Chap. **5,** New York: Academic Press 1974
28. Anderson, S. K.: Graph theory and finite combinatorics, Chap. 1. Chicago: Markham Publishing Co. 1970
29. Roberts, F. S.: Discrete mathematical models. Englewood Cliffs, New Jersey: Prentice-Hall 1976
30. Wilson, R. J.: Introduction to graph theory, p. 16. Edinburgh: Oliver and Boyd. 1972
31. Harary, F., in: Graph theory and theoretical physics, p. 4. Harary, F., Ed. New York: Academic Press 1967
32. Higgins, J.: Ind. and Eng. Chem. **59,** p. 32, Fig. 10 (1967)
33. Biggs, N. L.: Algebraic graph theory, Chap. 2. London: Cambridge University Press 1974
34. Tyson, J. J.: J. Chem. Phys. **62,** 1010 (1975)
35. May, R. M.: Stability and complexity in model ecosystems. Princeton, N. J.: Princeton University Press 1973
36. Glandsdorff, P., Prigogine, I.: Thermodynamic theory of structure, stability, and fluctuations. New York: Wiley 1971
37. Nicolis, G.: Advan. Chem. Phys. **19,** 209 (1971)
38. Tyson, J. J.: J. Chem. Phys. **58,** 3919 (1973)
39. Lorenz, E. N.: J. Atmos. Sci. **20,** 130 (1963)
40. Collatz, L., Sinogowitz, U.: Abh. Math. Sem. Univ. Hamburg **21,** 63 (1957)
41. Biggs, N. L.: Algebraic graph theory, Chap. 7. London: Cambridge University Press 1974
42. Conkwright, N. B.: Introduction to the theory of equations, Chap. 5. Boston: Ginn and Co. 1941

Received February 1, 1980